



**University of  
Zurich<sup>UZH</sup>**

**Zurich Open Repository and  
Archive**

University of Zurich  
University Library  
Strickhofstrasse 39  
CH-8057 Zurich  
[www.zora.uzh.ch](http://www.zora.uzh.ch)

---

Year: 2014

---

**Assessment of ischaemic burden in angiographic three-vessel coronary artery disease with high-resolution myocardial perfusion cardiovascular magnetic resonance imaging**

Motwani, M ; Maredia, N ; Fairbairn, T A ; Kozerke, S ; Greenwood, J P ; Plein, S

DOI: <https://doi.org/10.1093/ehjci/jet286>

Posted at the Zurich Open Repository and Archive, University of Zurich

ZORA URL: <https://doi.org/10.5167/uzh-98643>

Journal Article

Published Version

Originally published at:

Motwani, M; Maredia, N; Fairbairn, T A; Kozerke, S; Greenwood, J P; Plein, S (2014). Assessment of ischaemic burden in angiographic three-vessel coronary artery disease with high-resolution myocardial perfusion cardiovascular magnetic resonance imaging. *European Heart Journal Cardiovascular Imaging*, 15(6):701-708.

DOI: <https://doi.org/10.1093/ehjci/jet286>

# Assessment of ischaemic burden in angiographic three-vessel coronary artery disease with high-resolution myocardial perfusion cardiovascular magnetic resonance imaging

Manish Motwani<sup>1</sup>, Neil Maredia<sup>1</sup>, Timothy A. Fairbairn<sup>1</sup>, Sebastian Kozerke<sup>2</sup>, John P. Greenwood<sup>1</sup>, and Sven Plein<sup>1\*</sup>

<sup>1</sup>Multidisciplinary Cardiovascular Research Centre & The Division of Cardiovascular and Diabetes Research, Leeds Institute of Genetics, Health and Therapeutics, University of Leeds, Leeds LS2 9JT, UK; and <sup>2</sup>Institute for Biomedical Engineering, University and ETH Zurich, Zurich, Switzerland

Received 29 September 2013; accepted after revision 17 December 2013; online publish-ahead-of-print 3 February 2014

## Aims

This study compared the myocardial ischaemic burden (MIB) in patients with angiographic three-vessel coronary artery disease (3VD) using high-resolution and standard-resolution myocardial perfusion cardiovascular magnetic resonance (perfusion CMR) imaging.

## Methods and results

One hundred and five patients undergoing coronary angiography had two separate stress/rest perfusion CMR studies, one with standard-resolution (2.5 mm in-plane) and another with high-resolution (1.6 mm in-plane). Quantitative coronary angiography was used to define patients with angiographic 3VD. Perfusion CMR images were anonymized, randomly ordered and visually reported by two observers acting in consensus and blinded to all clinical and angiographic data. Perfusion was graded in each segment on a four-point scale and summed to produce a perfusion score and estimate of MIB for each patient. In patients with angiographic 3VD ( $n = 35$ ), high-resolution acquisition identified more abnormal segments ( $7.2 \pm 3.8$  vs.  $5.3 \pm 4.0$ ;  $P = 0.004$ ) and territories ( $2.4 \pm 0.9$  vs.  $1.6 \pm 1.1$ ;  $P = 0.002$ ) and a higher overall perfusion score ( $20.1 \pm 7.7$  vs.  $11.9 \pm 9.4$ ;  $P < 0.0001$ ) per patient compared with standard-resolution. The number of segments with subendocardial ischaemia was greater with high-resolution acquisition (195 vs. 101;  $P < 0.0001$ ). Hypoperfusion in all three territories was identified in 57% of 3VD patients by high-resolution compared with only 29% by standard-resolution ( $P = 0.04$ ). The area-under-the-curve (AUC) for detecting angiographic 3VD using the estimated MIB was significantly greater with high-resolution than standard-resolution acquisition (AUC = 0.90 vs. 0.69;  $P < 0.0001$ ).

## Conclusion

In patients with angiographic 3VD, the ischaemic burden detected by perfusion CMR is greater with high-resolution acquisition due to better detection of subendocardial ischaemia. High-resolution perfusion CMR may therefore be preferred for risk stratification and management of this high-risk patient group.

## Keywords

coronary artery disease • magnetic resonance imaging • ischaemia • myocardial perfusion imaging

## Introduction

Three-vessel coronary artery disease (3VD) is found in ~9% of patients undergoing elective coronary angiography and these patients have a considerably poorer prognosis than those with less

extensive disease.<sup>1</sup> Detection of 3VD with non-invasive imaging can be challenging due to the effects of balanced ischaemia leading to false-negative results in up to 20% of cases.<sup>2,3</sup> This limitation has been well documented with single-photon emission computed tomography (SPECT), and although its overall sensitivity for detecting

\* Corresponding author. Tel: +44 113 3437720; Fax: +44 113 3436603, Email: s.plein@leeds.ac.uk

© The Author 2014. Published by Oxford University Press on behalf of the European Society of Cardiology.

This is an Open Access article distributed under the terms of the Creative Commons Attribution Non-Commercial License (<http://creativecommons.org/licenses/by-nc/3.0/>), which permits non-commercial re-use, distribution, and reproduction in any medium, provided the original work is properly cited. For commercial re-use, please contact [journals.permissions@oup.com](mailto:journals.permissions@oup.com)

coronary artery disease (CAD) in multi-vessel disease is 80–95%, it often only detects perfusion defects in one territory.<sup>2,4,5</sup> In one SPECT study, inducible perfusion abnormalities in all three territories were identified in only 12% of patients with known angiographic 3VD.<sup>6</sup>

Myocardial perfusion cardiovascular magnetic resonance (perfusion CMR) imaging is a highly accurate method for the detection of significant CAD.<sup>7–9</sup> One of the major advantages of perfusion CMR compared with SPECT is its higher spatial resolution (typically 2–3 vs. 8–10 mm). Balanced ischaemia can lead to diffuse subendocardial hypoperfusion and although there are few comparisons between perfusion CMR and SPECT in 3VD, it is expected that the higher resolution of CMR can better resolve the transmural perfusion gradient in balanced ischaemia and thereby potentially improve the detection of 3VD.<sup>10</sup> With recently developed spatio-temporal undersampling methods such as *k-t* broad-use linear acquisition speed-up technique (*k-t* BLAST), the spatial resolution of perfusion CMR can be improved further to <2 mm.<sup>11</sup>

Several studies have demonstrated the feasibility and accuracy of high-resolution perfusion CMR.<sup>12–16</sup> In a direct comparison, we have previously shown that high-resolution perfusion CMR has a higher overall diagnostic accuracy compared with standard-resolution imaging in patients with suspected CAD. This previous study included a small subset of patients with multi-vessel disease.<sup>16</sup> The present study aims to compare the distribution of and extent of ischaemia in patients with 3VD detected by both techniques and tests the hypothesis that improved performance of high-resolution CMR is due to better detection of subendocardial ischaemia in 3VD.

## Methods

### Study population

A total of 105 patients were included in this analysis. All had undergone coronary angiography for suspected angina within the last 30 days. Seventy patients were prospectively recruited: 35 had 3VD on quantitative coronary angiography and 35 with normal coronary arteries served as a control group. Data from 24 of the patients with angiographic 3VD have been previously reported with different endpoints (diagnostic accuracy rather than pattern of ischaemia or ischaemic burden).<sup>16</sup> Additionally, we selected 35 consecutive patients with angiographic 1VD or 2VD from the same previous study to prevent a spectrum bias for the secondary analyses relating to myocardial ischaemic burden (MIB).<sup>16</sup> Exclusion criteria for all patients were contra-indications to CMR, adenosine, or gadolinium contrast agent; or a history of recent (within 6 months) myocardial infarction (MI), unstable angina, or revascularization. Additionally, patients with angiographic 1VD or 2VD and co-existing moderate coronary artery stenoses (i.e. 40–69%) in other territories were not included. All patients gave written consent and the study was approved by the regional ethics committee.

### CMR protocol

All patients underwent a standard-resolution and a high-resolution perfusion scan on separate days (within 4 weeks) using a 1.5-T scanner (Intera, Philips Healthcare, Best, The Netherlands).

The standard perfusion pulse sequence was a saturation recovery gradient-echo method accelerated with sensitivity encoding (SENSE) (SENSE acceleration factor 2, repetition time (TR) 2.7 ms, echo time (TE) 1.0 ms, flip-angle = 15°, acquisition time per slice = 136 ms, single-saturation pre-pulse per R–R interval shared over three slices, matrix =

144 × 144, median field-of-view (FOV) = 360 mm, in-plane spatial resolution = 2.5 mm). The high-resolution perfusion pulse sequence used a similar saturation recovery gradient-echo method, but was accelerated with *k-t* BLAST (acceleration factor 8 with 11 training profiles, TR = 3.4 ms, TE = 1.7 ms, flip-angle = 15°, one saturation pre-pulse per slice, acquisition time per slice = 103 ms, matrix = 192 × 192, median FOV = 310 mm, in-plane spatial resolution = 1.6 mm). For both techniques, perfusion data were acquired in three short-axis slices in each R–R interval.

For both studies, stress perfusion started after 4 min of an intravenous adenosine infusion (140 mcg/kg/min) during an intravenous bolus injection of dimeglumine gadopentetate (Magnevist; Schering AG, West Sussex, UK) and a 15-mL saline flush delivered at 5 mL/s. Contrast dose and administration protocols for both studies were chosen to optimize their visual analysis performance based on their use in previous studies. For the standard-resolution method, a contrast dose of 0.05 mmol/kg body weight was used during perfusion acquisition, identical to previous studies with this pulse sequence.<sup>9,16</sup> To compensate for the lower signal-to-noise ratio (SNR) associated with smaller voxel size, a contrast dose of 0.1 mmol/kg body weight was used for the high-resolution method, consistent with previous reports.<sup>13,14,16,17</sup>

Rest perfusion imaging was performed 15 min later. Late gadolinium-enhancement (LGE) imaging was performed in all patients on their first visit using conventional methods (1.6 mm in-plane spatial resolution) and a cumulative contrast dose of 0.2 mmol/kg body weight (the same for both protocols). During standard-resolution perfusion CMR scans, this cumulative dose was achieved by administration of an additional contrast bolus of 0.1 mmol/kg body weight immediately after rest perfusion.

### CMR analysis

CMR images were anonymized, randomly ordered and visually reported by two observers (S.P. and M.M., 10 and 2 years experience, respectively) acting in consensus and blinded to all clinical and angiographic data (QMASS 6.1.6, Medis, Leiden, The Netherlands). In case of disagreement, arbitration from a third observer was sought (J.P.G., 10 years experience). Using a 16-segment model, perfusion in a segment was considered abnormal if signal intensity was reduced compared with remote myocardium or an endocardial-to-epicardial perfusion gradient was present.<sup>12,18</sup> Additionally, any perfusion defect was required to persist beyond the peak myocardial signal enhancement to distinguish it from artefact. Corresponding LGE images were reviewed side-by-side with the perfusion data. Perfusion defects present at stress but not rest and occurring outside any hyperenhanced myocardial tissue on LGE images were considered as inducible defects. Perfusion in each segment was graded on a four-point scale (transmural ischaemia index: 0 = normal, 1 = inconclusive, 2 = subendocardial defect, 3 = transmural defect). A typical example of perfusion images is seen in Figure 1. All segmental scores were summed to produce a perfusion score (0–48) for each patient. MIB as a percentage of the total myocardium (MIB%) was estimated by dividing the perfusion score by 48 and multiplying by 100.<sup>19</sup> In patients with 3VD, perfusion scores were also calculated for the left anterior descending (LAD), left circumflex (LCX) and right coronary artery (RCA) territories according to american heart association (AHA) segmentation adjusted for arterial dominance.<sup>18</sup>

Image quality was graded 1–4 (1 = unusable, 2 = poor, 3 = adequate, 4 = excellent). Occurrence of artefacts related to *k-t* reconstruction, respiratory motion, electrocardiographic gating, and endocardial dark-rim was scored 0–3 (0 = none, 1 = minor, 2 = moderate, 3 = severe). Where present, the width of dark-rim artefact (DRA) (a frequent finding in perfusion CMR at the myocardial–blood pool interface relating to cardiac motion, Gibb's ringing, susceptibility, and partial volume cancellation) was measured with electronic callipers.<sup>16,20</sup>

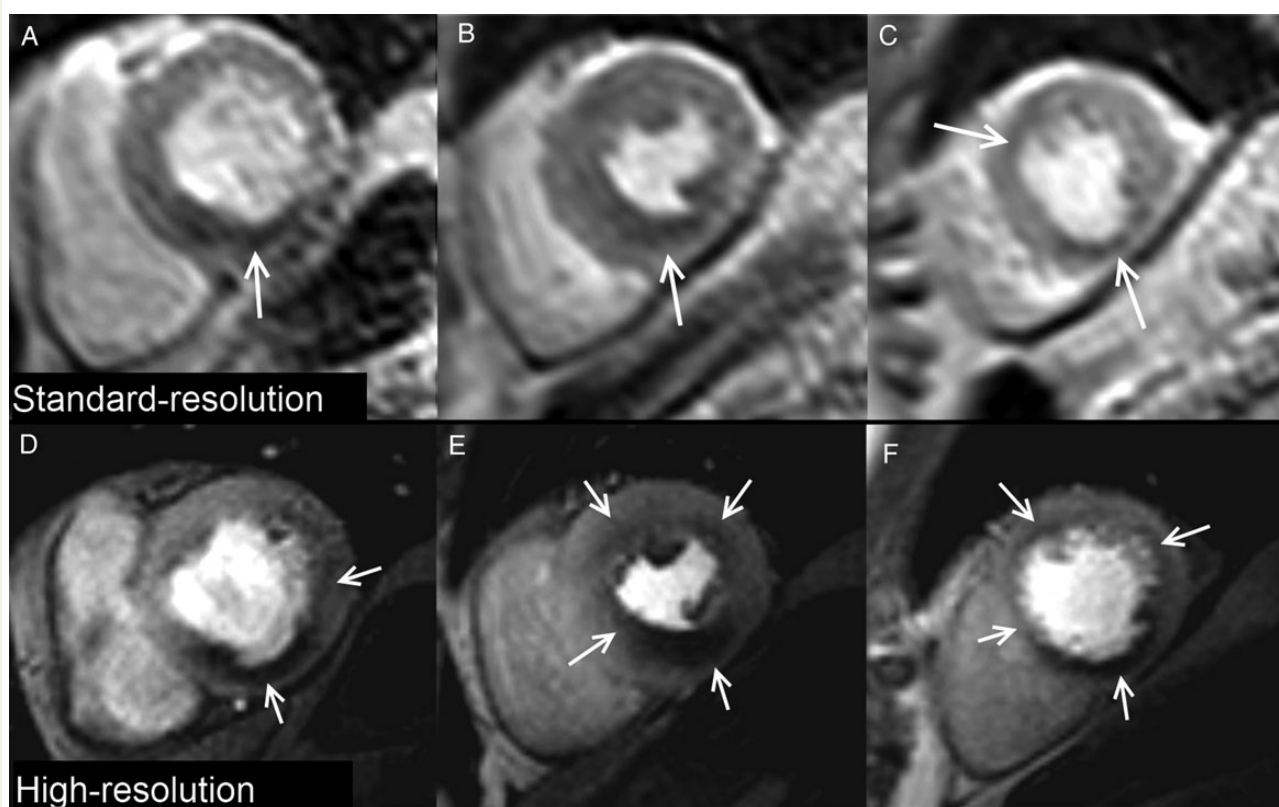


**Figure 1** Case example. Standard and high-resolution stress perfusion CMR in a patient with three-vessel coronary artery disease. Standard-resolution shows perfusion defects (arrows) in the basal-inferior (A), mid-inferior, mid-inferoseptal (B), apical-anterior and apical-inferior segments (C). High-resolution shows a similar distribution of perfusion defects but demonstrates additional ischaemia in the basal-lateral (D), mid-anterior, and mid-anterolateral segments (E) with a circumferential defect in the apical slice (F). Perfusion defects are also better delineated at high-resolution and the transmural extent of ischaemia more clearly seen.

## Quantitative coronary angiography

Quantitative coronary angiography (QCA) was performed (QCAPlus, Sanders Data Systems, Palo Alto, CA, USA) by an experienced observer blinded to CMR data (M.M., 7 years of experience in coronary angiography). Stenoses were assigned to the appropriate myocardial segments of an AHA 16-segment model using standard criteria adjusted for arterial dominance and lesion location.<sup>18,21</sup> As per convention, significant CAD was defined as luminal stenosis  $\geq 70\%$  in any of the major epicardial coronary arteries or first-order branches  $\geq 2$  mm. Angiographic 3VD was defined as stenosis  $\geq 70\%$  in all three coronary arteries; or the presence of  $\geq 50\%$  stenosis in the left main stem with  $\geq 70\%$  in the RCA. Normal coronary arteries were defined as an absence of any stenosis  $\geq 40\%$ . Collateral circulation was graded according to the Rentrop classification (RC) depending on the angiographic findings of the occluded artery using the best injection: 0 = no collateral circulation; 1 = collateral filling of side branches without visualization of any epicardial segments; 2 = collaterals partially filling the epicardial segment; 3 = collaterals completely filling the epicardial segment.<sup>22</sup>

## Statistical analysis

Analysis was performed using SPSS 17.0 (SPSS, Chicago, IL, USA). Mean values were compared using paired Student *t*-tests. Ordinal data were compared using  $\chi^2$  or Wilcoxon signed-rank tests as appropriate.

Paired proportions were compared using McNemar's exact test. The pattern of ischaemia determined by both techniques for patients with angiographic 3VD was compared using Cohen's kappa statistic. MIB% was compared across 1VD, 2VD, and 3VD groups using one-way analysis of variance and Tukey's *post hoc* test. Receiver-operator characteristic (ROC) curve analyses were performed on summed perfusion scores for individual territories and on MIB% per patient. Area-under-the-curve (AUC) for both imaging techniques were compared using methods described by DeLong and DeLong. All tests were two-tailed and  $P < 0.05$  was considered statistically significant.

## Results

### Study population

A total of 105 patients were enrolled into the study, including 35 with 3VD by QCA. Of these 35 patients, 32 qualified as angiographic 3VD on the basis of significant stenoses in the proximal coronary segments and no patients qualified as angiographic 3VD on the basis of distal coronary segment disease. Further demographics are given in Table 1. All 14 patients with a clinical history of MI (but no additional patients) had evidence of hyperenhancement on LGE imaging. A chronic total occlusion (CTO) was seen in six patients (all in the

**Table 1** Patient clinical characteristics (n = 105)

Age, years	68 ± 10
Males	75 (71)
Medical history	
Hypertension	65 (62)
Hypercholesterolaemia	62 (59)
Diabetes mellitus	18 (17)
Smoking	43 (41)
Family history of CAD	39 (37)
Previous MI	14 (13)
Previous PCI	10 (9)
Atrial fibrillation	1 (1)
LV ejection fraction, %	55 ± 11
Angiography findings <sup>a</sup>	
No significant disease	35 (33)
One-vessel disease	25 (24)
Two-vessel disease	10 (9)
Three-vessel disease	35 (33)
LAD disease	51 (49)
LCX disease	50 (48)
RCA disease	49 (47)
Significant lesions per patient	1.4 ± 1.2
Total significant lesions	150
70–90% stenoses	109 (73)
90–99% stenoses	35 (23)
Chronic total occlusions	6 (4)

Values are mean ± SD or n (%). MI, myocardial infarction; PCI, percutaneous coronary intervention; LAD, left anterior descending coronary artery; LCX, left circumflex coronary artery; RCA, right coronary artery.  
<sup>a</sup>Significant coronary artery disease (CAD) defined as coronary stenosis ≥70% on quantitative coronary analysis.

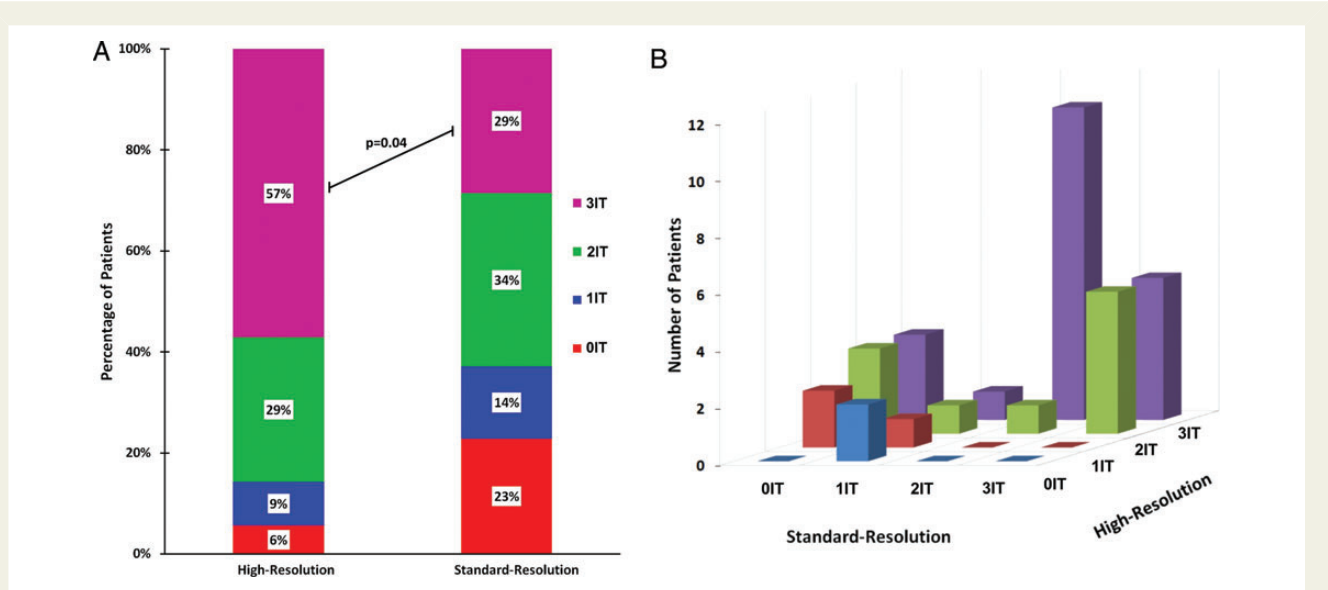
group with prior MI) and two of these patients were in the 3VD group. There were no patients with more than one CTO. In two cases of CTO (neither in the 3VD group) there was mild collateral flow (RC = 2), but in the remaining four cases there was no or minimal collateralization (RC ≤ 1).

Image quality and artefacts

There was no significant difference in the haemodynamic stress response during standard- and high-resolution imaging (rate–pressure product, mmHg × beats/min: 10 251 ± 2321 vs. 10 201 ± 2109; *P* = 0.92). No images were graded as unusable and therefore there were no exclusions from the image analysis for either technique. Image quality (median score = 3 for both; *P* = 0.67) and artefact scores (median = 0 for both; *P* = 0.06) were similar for both standard- and high-resolution imaging across the full spectrum of patients (*n* = 105). DRA was significantly less frequent with high-resolution (7% vs. 26%; *P* = 0.03) and when it did occur, it was less marked than with standard-resolution (1.6 ± 0.2 vs. 3.2 ± 0.8 mm; *P* = 0.004). Seven high-resolution data sets (10%) were affected by *k*-*t* reconstruction artefacts at stress and/or rest due to respiratory motion, but this did not affect myocardial contrast passage and generally occurred at the end of a breath hold.

Detection of 3VD pattern

In patients with angiographic 3VD (*n* = 35), perfusion defects in all three territories were detected in 29% of patients (10 of 35) by standard-resolution and in 57% of patients (20 of 35) by high-resolution imaging (*P* = 0.04) (Figure 2A). Overall, there was poor agreement between the two techniques in determining the pattern of ischaemia in patients with angiographic 3VD [kappa = 0.09, 95% confidence interval (CI): −0.10–0.29] (Figure 2B).



**Figure 2** Distribution of ischaemia detected by perfusion CMR. (A) In patients with 3VD (*n* = 35), hypoperfusion in all three territories was detected in 57% using high-resolution imaging but in only 29% using standard-resolution (*P* = 0.04). (B) There was also poor agreement between high-resolution and standard-resolution imaging in determining the distribution of ischaemia in patients with 3VD (kappa = 0.09, 95% CI: −0.10–0.29). IT = ischaemic territories.



**Table 2** Diagnostic performance of perfusion CMR in each territory in patients with 3VD

	AUC (95% CI)		P-value
	Standard-resolution	High-resolution	
LAD	0.82 (0.69–0.95)	0.85 (0.73–0.97)	0.62
LCX	0.62 (0.46–0.79)	0.83 (0.70–0.95)	0.02
RCA	0.83 (0.70–0.95)	0.90 (0.80–1.00)	0.27

## Detection of CAD in each territory

In patients with angiographic 3VD ( $n = 35$ ), separate ROC analyses of perfusion scores for each of the three coronary territories were performed. The AUC for each territory in patients with angiographic 3VD was greater with high-resolution than with standard-resolution imaging, but reached statistical significance only for the LCX territory (Table 2).

With standard-resolution imaging, diagnostic accuracy was significantly lower for the LCX than for the LAD (0.62 vs. 0.82;  $P < 0.01$ ) or RCA territory (0.62 vs. 0.83;  $P = 0.02$ ). With high-resolution, diagnostic accuracies were more homogenous between territories (although still lowest in the LCX territory) with no statistical difference between them (LAD: 0.85 vs. LCX: 0.83 vs. RCA: 0.90; all  $P$ -values  $> 0.05$ ).

## Detection of subendocardial ischaemia

Five hundred and sixty myocardial segments were available from the 35 patients with angiographic 3VD. Of these, 420 were determined as angiographically hypoperfused and used for further analysis. With high-resolution acquisition, significantly more of these hypoperfused segments were determined as having subendocardial ischaemia than with standard-resolution (195 vs. 101;  $P < 0.0001$ ); and there was a significant reduction in the number of segments determined as being normal (135 vs. 212;  $P < 0.001$ ) or inconclusive (15 vs. 40;  $P < 0.001$ ). The number of segments assessed as having transmural ischaemia was similar with both techniques (75 vs. 67;  $P = 0.25$ ) (Figure 3).

## Detection of ischaemic burden

In patients with angiographic 3VD ( $n = 35$ ), the overall extent of myocardial ischaemia detected was significantly greater with high-resolution than standard-resolution imaging, with more abnormal segments per patient ( $7.2 \pm 3.8$  vs.  $5.3 \pm 4.0$ ;  $P = 0.004$ ), more abnormal territories per patient ( $2.4 \pm 0.9$  vs.  $1.6 \pm 1.1$ ;  $P = 0.002$ ), a higher perfusion score per territory ( $5.9 \pm 4.3$  vs.  $4.7 \pm 5.0$ ;  $P = 0.01$ ) and a higher overall perfusion score per patient ( $20.1 \pm 7.7$  vs.  $11.9 \pm 9.4$ ;  $P < 0.0001$ ) (Figure 1 and Table 3).

When the full spectrum of 105 patients were assessed, high-resolution imaging found a significant upward trend in estimated MIB% in those with significant CAD ( $n = 70$ ) across advancing disease groups (1VD:  $12 \pm 7\%$  vs. 2VD:  $39 \pm 15\%$  vs. 3VD:  $42 \pm 16\%$ ;  $P < 0.0001$ ).<sup>16</sup> However, with standard-resolution, there was no discriminate difference in estimated MIB% across the disease groups (1VD:  $21 \pm 11\%$  vs. 2VD:  $25 \pm 6\%$  vs. 3VD:  $25 \pm 19\%$ ;  $P = 0.53$ ) (Figure 4A).

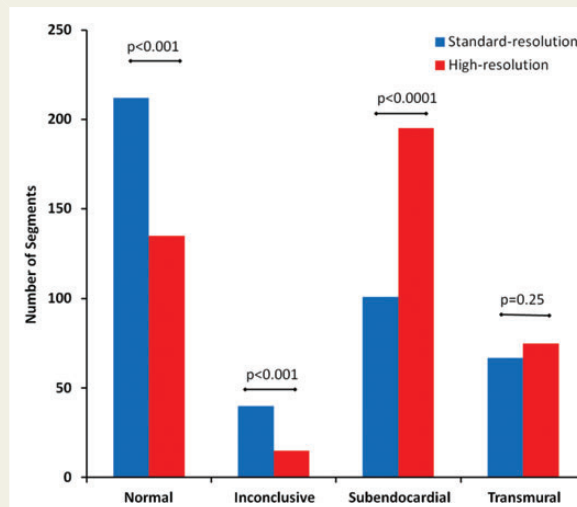


**Figure 3** Distribution of transmural ischaemia index. In patients with three-vessel disease ( $n = 35$ ), high-resolution perfusion CMR determined significantly more segments as having subendocardial ischaemia and fewer as normal or inconclusive compared with standard-resolution imaging.

**Table 3** Detection of ischaemic burden with perfusion CMR in patients with 3VD

	Standard-resolution	High-resolution	P-value
Mean abnormal segments per patient	$5.3 \pm 4.0$	$7.2 \pm 3.8$	0.004
Mean abnormal territories per patient	$1.6 \pm 1.0$	$2.4 \pm 0.9$	0.002
Mean perfusion score per patient	$11.9 \pm 9.4$	$20.1 \pm 7.7$	$< 0.0001$
Mean perfusion score per territory	$4.7 \pm 5.0$	$5.9 \pm 4.3$	0.01

Accordingly, on ROC analysis, the AUC for detecting angiographic 3VD using the estimated MIB% was significantly greater with high-resolution (AUC = 0.90, 95% CI: 0.84–0.96) than standard-resolution (AUC = 0.69, 95% CI: 0.62–0.76;  $P < 0.0001$ ) (Figure 4B) imaging. For high-resolution imaging the optimal MIB% threshold to detect angiographic 3VD was 31% which resulted in a sensitivity and specificity of 80% (95% CI: 64–90%) and 90% (95% CI: 80–95%), respectively. For standard-resolution imaging, the optimal threshold was 23%, which resulted in a sensitivity and specificity of 51% (95% CI: 36–67%) and 78% (95% CI: 66–86%), respectively (Figure 4B).

## Discussion

This study shows that in patients with angiographic 3VD, high-resolution perfusion CMR detects a greater ischaemic burden than

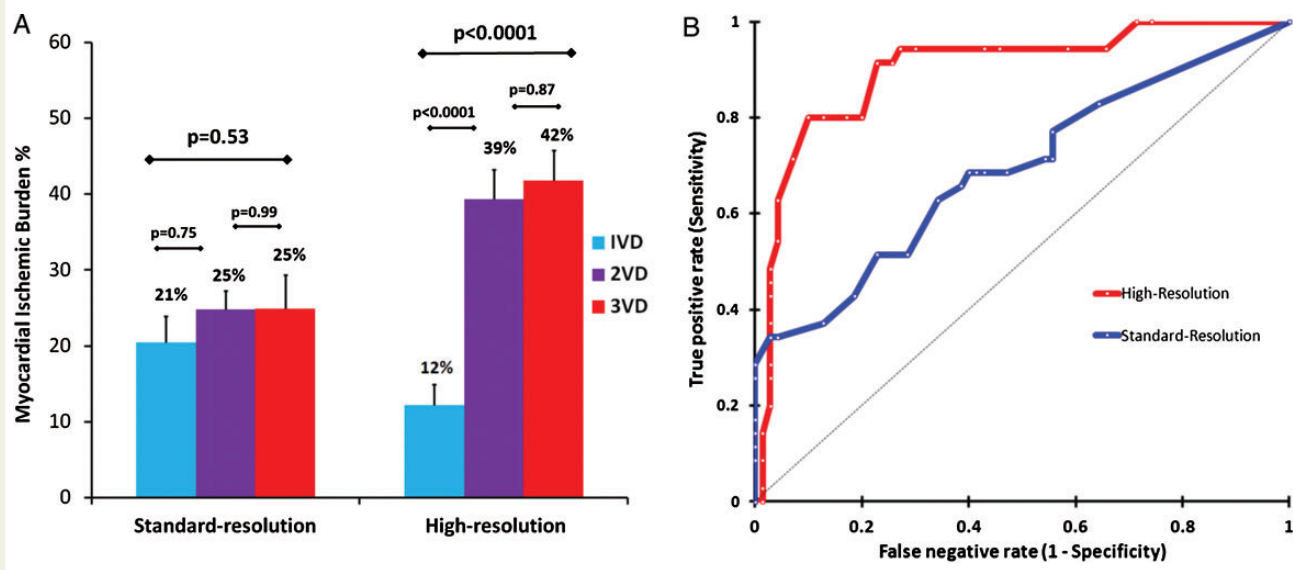


**Figure 4** Myocardial ischaemic burden (MIB). (A) In patients with significant coronary artery disease ( $n = 70$ ), high-resolution perfusion CMR was able to detect significant differences in MIB across disease categories unlike standard-resolution imaging (error bars = SEM). (B) The AUC for detecting 3VD using MIB among patients with suspected angina ( $n = 105$ ) was significantly greater with high-resolution than standard-resolution (AUC = 0.90 vs. 0.69;  $P < 0.0001$ ). VD = vessel disease.

standard-resolution and more frequently identifies a 3VD pattern of ischaemia due to a higher detection rate of subendocardial ischaemia.

The evidence for using perfusion CMR in patients with 3VD is limited. Although previous studies evaluating perfusion CMR have included patients with 3VD, they have rarely reported separate results for this specific patient population. In the published data, the incidence of patients with 3VD was only 2% (2 patients) in the study by Sakuma *et al.*, 15% (8 patients) in the study by Ishida *et al.*, and 19% (7 patients) in the study by Schwitter *et al.*<sup>8,23,24</sup> Although other studies may contain larger numbers, patients with 3VD are rarely analysed separately and they are usually grouped together with patients found to have 2VD.<sup>7,9,25</sup> Only one study to date has been specifically designed to evaluate standard-resolution perfusion CMR in patients with 3VD ( $n = 78$ ) and it demonstrated a sensitivity of 85% for CAD detection and superiority of perfusion CMR compared with SPECT.<sup>6</sup> Data on the use of high-resolution perfusion CMR in the specific 3VD population are even scarcer. However, in a recent related analysis, we reported on 38 patients with angiographic multi-vessel disease (24 had 3VD) and found a greater diagnostic accuracy for the detection of CAD (any perfusion defect) with high-resolution perfusion CMR compared with standard-resolution imaging (AUC, 0.98 vs. 0.91;  $P < 0.002$ ), but the pattern of perfusion defects detected and the ischaemic burden were not assessed.<sup>16</sup>

## Detection of subendocardial ischaemia

The finding in the present study indicates that high-resolution acquisition identified significantly more ischaemic segments and in particular more segments with subendocardial ischaemia in angiographic 3VD is consistent with the expected improvement in subendocardial definition with higher spatial resolution. Although we have previously demonstrated this finding across the full spectrum of CAD, it was

important to confirm that this advantage is maintained in the 3VD population against the competing challenge of balanced ischaemia.<sup>16</sup> It means that one of the major limitations of myocardial perfusion imaging and visual analysis in 3VD, i.e. its dependence on a reference area of normal perfusion, can be overcome to some extent with high-resolution techniques that are able to resolve subendocardial ischaemia and transmural perfusion gradients, reducing the need for intra-patient comparison. An alternative approach is *quantitative* analysis of standard perfusion CMR and although this has been shown to identify patients with 3VD better than visual analysis, it remains a time-consuming research tool until technical developments lead to greater automation.<sup>21</sup> The significant reduction of DRA with high-resolution may also partially account for its improved detection of subendocardial ischaemia and notably there were fewer inconclusive segments with high-resolution acquisition compared with standard-resolution (Figure 3). Previous work investigating DRA has shown the prominent role of spatial resolution on the occurrence and extent of this artefact.<sup>17,20</sup>

## Detection of 3VD pattern

Standard-resolution perfusion CMR identified defects in all three perfusion territories in only 29% of patients with angiographic 3VD (10 of 35) (Figure 2B). In the published CMR literature, there is only one study that investigates the same question and it found a significantly greater figure of over 50% using standard-resolution techniques.<sup>6</sup> However, this previous retrospective study only analysed patients with 3VD, without a control group; and additionally did not use LGE imaging to exclude areas of infarction from inducible ischaemia, both of which are likely to have led to a positive bias. In the comparative SPECT literature, we see the ability to detect a 3VD

pattern is similarly only 29% in one series and as low as 12% in another.<sup>2,6</sup>

With the high-resolution perfusion CMR method, twice as many patients with angiographic 3VD, i.e. 57% (20 of 35) were correctly classified as having a 3VD pattern of ischaemia (Figure 2B). The improved detection of a 3VD pattern of ischaemia with high-resolution compared with standard-resolution acquisition was due to better detection of ischaemia in the LCX territory and more sub-endocardial ischaemia detection. Disease of the LCX territory can be difficult to detect because this territory is farthest from the radiofrequency coil and because visual, unlike quantitative assessment analysis, cannot correct signal intensity for distance from the coil.<sup>6,26</sup> In keeping with previous studies, high-resolution acquisition used a higher contrast dose (in order to compensate for the lower SNR associated with smaller voxel size) and arguably this may have contributed to its superior performance in the LCX territory.<sup>13,14,16,17</sup>

Rather than inadequacy of the perfusion analysis, the low detection rate of ischaemia in multiple territories by different imaging modalities may reflect at least in part the inadequacy of the purely anatomical angiographic endpoint in these studies including our own. In a sub-analysis of the FAME study, only 14% of patients with angiographic 3VD ( $n = 115$ ) had concordant three-vessel functional disease determined by fractional flow reserve (FFR) (i.e.  $\text{FFR} < 0.80$  in all three vessels).<sup>27</sup>

## Estimation of ischaemic burden

It can be argued that in clinical practice, it is less relevant whether a functional scan depicts a typical three-vessel pattern if there is myocardial ischaemia involving a significant proportion of total myocardium. An accurate assessment of ischaemic burden is important because the extent of ischaemia is a marker of patient prognosis—and a large ischaemic burden supports aggressive medical treatment and angiography with a view to revascularization regardless of the territorial pattern of perfusion defect.<sup>19,28–30</sup> When MIB% was estimated using high-resolution CMR, it was found to reliably discriminate angiographic 3VD from less extensive disease and normal controls ( $\text{AUC} = 0.89$ ) (Figure 4). This was not the case for standard-resolution CMR, for which MIB% had a significantly poorer diagnostic accuracy ( $\text{AUC} = 0.69$ ;  $P < 0.0001$ ) and was not able to reliably differentiate between patients with 1VD, 2VD, or 3VD (Figure 4). The latter observation regarding standard-resolution perfusion CMR has been previously noted by Patel *et al.*<sup>21</sup> who found similar estimates of ischaemic burden in patients with angiographic single-vessel disease and 3VD with visual assessment (21% vs. 31%;  $P = 0.26$ ), but a significant difference if quantified with myocardial perfusion reserve analysis (25% vs. 60%;  $P = 0.02$ ). A similar phenomenon has been described with positron emission tomography.<sup>31</sup> High-resolution perfusion CMR acquisition appears to overcome this limitation seen with lower spatial resolution imaging methods.

Although there is no agreed reference standard for MIB%, the current data suggest that standard-resolution imaging underestimates MIB%—and this should be considered in the interpretation of future perfusion CMR studies that may use a particular threshold of ischaemic burden as a defined end-point or inclusion criteria. In the nuclear sub-study of COURAGE, patients with a  $\text{MIB\%} > 10\%$  had a lower risk of death or MI if they underwent revascularization rather than optimal medical therapy alone.<sup>30</sup> Notably, there has

been no direct comparison of CMR and SPECT for MIB% assessment—but if the threshold defined for SPECT is applied to the CMR data in this study, 24 of 35 patients with angiographic 3VD had an  $\text{MIB\%} > 10\%$  using standard-resolution perfusion CMR, compared with 33 patients with the high-resolution technique. Thus, high-resolution perfusion CMR may offer an improved non-invasive assessment of ischaemic burden and help identify the optimal therapeutic approach.

## Study limitations

Our findings are mainly technical, and further studies with clinical outcome data would be required to support the proposed incremental value of high-resolution perfusion CMR. We also accept that although we hypothesize the superior performance of high-resolution perfusion CMR relates to greater spatial resolution and better detection of sub-endocardial ischaemia, we cannot exclude the influence of other factors such as differences in SNR between scans and the difference in contrast protocols used as compensation.

A functional endpoint such as FFR would have been preferable—but this is not easily achievable given the logistics of performing multiple FFR assessments on serial and complex stenoses in three diffusely diseased arteries to define each subject. However, our findings predominantly relate to comparative differences in ischaemic burden assessment between the two techniques rather than their absolute ability to detect any ischaemia.

Because the visual CMR analysis was performed by two observers acting in consensus, inter-observer and intra-observer variability for perfusion scoring was not tested; however, arbitration from a third reader was only required in 5 out of the 210 analyses (3 with standard and 2 with high-resolution).

Finally, quantitative methods for the estimation of myocardial blood flow (MBF) based on perfusion CMR data have been validated in animal models and applied to clinical studies.<sup>21</sup> However, in this study, contrast agent dose and administration (single-bolus technique) were optimized for visual analysis and therefore quantitative analysis was not performed. Although high-resolution perfusion CMR offers further intriguing opportunities for quantitative analysis the algorithms applied for the reconstruction of high-resolution perfusion CMR data acquired with temporospatial undersampling methods give rise to a degree of low-pass temporal filtering, posing additional challenges to quantitation of MBF including an underestimation bias.<sup>32,33</sup> Recent developments such as  $k$ -t principal component analysis are likely to overcome some of these challenges but will require evaluation in future studies.<sup>34</sup>

## Conclusions

High-resolution perfusion CMR increases the observed ischaemic burden and distribution of ischaemia detected in angiographic 3VD. The incremental value of high-resolution acquisition for correctly identifying, stratifying, and managing this high-risk group has to be determined in further clinical studies.

## Acknowledgements

The authors thank Margaret Saysell, Caroline Richmond, and Gavin Bainbridge (radiographers) for their technical assistance; and Petra



Bijsterveld and Fiona Richards (research nurses) for their assistance with patient recruitment.

**Conflicts of interest:** none declared.

## Funding

S.P. is funded by British Heart Foundation fellowship (FS/10/62/28409). S.P. and J.P.G. received a research grant from Philips Healthcare. Funding to pay the Open Access publication charges for this article was provided by The British Heart Foundation.

## References

1. Emond M, Mock MB, Davis KB, Fisher LD, Holmes DR Jr, Chaitman BR et al. Long-term survival of medically treated patients in the Coronary Artery Surgery Study (CASS) Registry. *Circulation* 1994;**90**:2645–57.
2. Christian TF, Miller TD, Bailey KR, Gibbons RJ. Noninvasive identification of severe coronary artery disease using exercise tomographic thallium-201 imaging. *Am J Cardiol* 1992;**70**:14–20.
3. Martin VW, Tweddel A, Hutton I. Balanced triple-vessel disease: enhanced detection by estimated myocardial thallium uptake. *Nucl Med Commun* 1992;**13**:149–53.
4. Mahmarian JJ, Boyce TM, Goldberg RK, Cocanougher MK, Roberts R, Verani MS. Quantitative exercise thallium-201 single photon emission computed tomography for the enhanced diagnosis of ischemic heart disease. *J Am Coll Cardiol* 1990;**15**:318–29.
5. DePasquale EE, Nody AC, DePuey EG, Garcia EV, Pilcher G, Bredlau C et al. Quantitative rotational thallium-201 tomography for identifying and localizing coronary artery disease. *Circulation* 1988;**77**:316–27.
6. Chung SY, Lee KY, Chun EJ, Lee WW, Park EK, Chang HJ et al. Comparison of stress perfusion MRI and SPECT for detection of myocardial ischemia in patients with angiographically proven three-vessel coronary artery disease. *AJR Am J Roentgenol* 2010;**195**:356–62.
7. Schwitter J, Wacker CM, van Rossum AC, Lombardi M, Al-Saadi N, Ahlstrom H et al. MR-IMPACT: comparison of perfusion-cardiac magnetic resonance with single-photon emission computed tomography for the detection of coronary artery disease in a multicentre, multivendor, randomized trial. *Eur Heart J* 2008;**29**:480–9.
8. Sakuma H, Suzawa N, Ichikawa Y, Makino K, Hirano T, Kitagawa K et al. Diagnostic accuracy of stress first-pass contrast-enhanced myocardial perfusion MRI compared with stress myocardial perfusion scintigraphy. *AJR Am J Roentgenol* 2005;**185**:95.
9. Greenwood JP, Maredia N, Younger JF, Brown JM, Nixon J, Everett CC et al. Cardiovascular magnetic resonance and single-photon emission computed tomography for diagnosis of coronary heart disease (CE-MARC): a prospective trial. *Lancet* 2012;**379**:453–60.
10. Bache RJ, Schwartz JS. Effect of perfusion pressure distal to a coronary stenosis on transmural myocardial blood flow. *Circulation* 1982;**65**:928–35.
11. Tsao J, Boesiger P, Pruessmann KP. k-t BLAST and k-t SENSE: dynamic MRI with high frame rate exploiting spatiotemporal correlations. *Magn Reson Med* 2003;**50**:1031–42.
12. Plein S, Kozerke S, Suerder D, Luescher TF, Greenwood JP, Boesiger P et al. High spatial resolution myocardial perfusion cardiac magnetic resonance for the detection of coronary artery disease. *Eur Heart J* 2008;**29**:2148–55.
13. Plein S, Schwitter J, Suerder D, Greenwood JP, Boesiger P, Kozerke S. k-Space and Time Sensitivity Encoding—accelerated Myocardial Perfusion MR Imaging at 3.0 T: Comparison with 1.5 T. *Radiology* 2008;**249**:493–500.
14. Manka R, Vitanis V, Boesiger P, Flammer AJ, Plein S, Kozerke S. Clinical feasibility of accelerated, high spatial resolution myocardial perfusion imaging. *JACC Cardiovasc Imaging* 2010;**3**:710–7.
15. Lockie T, Ishida M, Perera D, Chiribiri A, Silva KDe, Kozerke S et al. High-resolution magnetic resonance myocardial perfusion imaging at 3.0-Tesla to detect hemodynamically significant coronary stenoses as determined by fractional flow reserve. *J Am Coll Cardiol* 2010;**57**:70–5.
16. Motwani M, Maredia N, Fairbairn TA, Kozerke S, Radjenovic A, Greenwood JP et al. High-resolution versus standard-resolution cardiovascular magnetic resonance myocardial perfusion imaging for the detection of coronary artery disease. *Circ Cardiovasc Imaging* 2012;**5**:306–13.
17. Plein S, Ryf S, Schwitter J, Radjenovic A, Boesiger P, Kozerke S. Dynamic contrast-enhanced myocardial perfusion MRI accelerated with k-t sense. *Magn Reson Med* 2007;**58**:777–85.
18. Cerqueira MD, Weissman NJ, Dilsizian V, Jacobs AK, Kaul S, Laskey WK et al. Standardized myocardial segmentation and nomenclature for tomographic imaging of the heart: a statement for healthcare professionals from the Cardiac Imaging Committee of the Council on Clinical Cardiology of the American Heart Association. *Circulation* 2002;**105**:539–42.
19. Hachamovitch R, Hayes SW, Friedman JD, Cohen I, Berman DS. Comparison of the short-term survival benefit associated with revascularization compared with medical therapy in patients with no prior coronary artery disease undergoing stress myocardial perfusion single photon emission computed tomography. *Circulation* 2003;**107**:2900–7.
20. Di Bella EV, Parker DL, Sinusas AJ. On the dark rim artifact in dynamic contrast-enhanced MRI myocardial perfusion studies. *Magn Reson Med* 2005;**54**:1295–9.
21. Patel AR, Antkowiak PF, Nandalur KR, West AM, Salerno M, Arora V et al. Assessment of advanced coronary artery disease advantages of quantitative cardiac magnetic resonance perfusion analysis. *J Am Coll Cardiol* 2010;**56**:561–9.
22. Rentrop KP, Cohen M, Blanke H, Phillips RA. Changes in collateral channel filling immediately after controlled coronary artery occlusion by an angioplasty balloon in human subjects. *J Am Coll Cardiol* 1985;**5**:587–92.
23. Ishida N, Sakuma H, Motoyasu M, Okinaka T, Isaka N, Nakano T et al. Noninfarcted myocardium: correlation between dynamic first-pass contrast-enhanced myocardial MR imaging and quantitative coronary angiography. *Radiology* 2003;**229**:209–16.
24. Schwitter J, Nanz D, Kneifel S, Bertschinger K, Büchi M, Knüsel PR et al. Assessment of myocardial perfusion in coronary artery disease by magnetic resonance: a comparison with positron emission tomography and coronary angiography. *Circulation* 2001;**103**:2230–5.
25. Schwitter J, Wacker CM, Wilke N, Al-Saadi N, Sauer E, Huettler K et al. MR-IMPACT II: Magnetic Resonance Imaging for Myocardial Perfusion Assessment in Coronary artery disease Trial: perfusion-cardiac magnetic resonance vs. single-photon emission computed tomography for the detection of coronary artery disease: a comparative multicentre, multivendor trial. *Eur Heart J* 2013;**34**:775–81.
26. Cheng AS, Pegg TJ, Karamitsos TD, Searle N, Jerosch-Herold M, Choudhury RP et al. Cardiovascular magnetic resonance perfusion imaging at 3-tesla for the detection of coronary artery disease: a comparison with 1.5-tesla. *J Am Coll Cardiol* 2007;**49**:2440–9.
27. Tonino PA, Fearon WF, De Bruyne B, Oldroyd KG, Leeser MA, Ver Lee PN et al. Angiographic versus functional severity of coronary artery stenoses in the FAME study fractional flow reserve versus Angiography in multivessel evaluation. *J Am Coll Cardiol* 2010;**55**:2816–21.
28. Hachamovitch R, Berman DS, Shaw LJ, Kiat H, Cohen I, Cabico JA et al. Incremental prognostic value of myocardial perfusion single photon emission computed tomography for the prediction of cardiac death: differential stratification for risk of cardiac death and myocardial infarction. *Circulation* 1998;**97**:535–43.
29. Wijns W, Kolh P, Danchin N, Di Mario C, Falk V, Folliquet T et al. Guidelines on myocardial revascularization: the Task Force on Myocardial Revascularization of the European Society of Cardiology (ESC) and the European Association for Cardio-Thoracic Surgery (EACTS). *Eur Heart J* 2010;**31**:2501–55.
30. Shaw LJ, Berman DS, Maron DJ, Mancini GBJ, Hayes SW, Hartigan PM et al. Optimal medical therapy with or without percutaneous coronary intervention to reduce ischemic burden results from the Clinical Outcomes Utilizing Revascularization and Aggressive Drug Evaluation (COURAGE) trial nuclear substudy. *Circulation* 2008;**117**:1283–91.
31. Parkash R, DeKemp RA, Ruddy TD, Kitsikis A, Hart R, Beauschene L et al. Potential utility of rubidium 82 PET quantification in patients with 3-vessel coronary artery disease. *J Nucl Cardiol* 2004;**11**:440–9.
32. Hautvast GLTF, Chiribiri A, Lockie T, Breeuwer M, Nagel E, Plein S. Quantitative analysis of transmural gradients in myocardial perfusion magnetic resonance images. *Magn Reson Med* 2011;**1487**:1477–87.
33. Jerosch-Herold M. Quantification of myocardial perfusion by cardiovascular magnetic resonance. *J Cardiovascular Magn Reson* 2010;**12**:57.
34. Pedersen H, Kozerke S, Ringgaard S, Nehrkne K, Kim WY. k-t PCA: temporally constrained k-t BLAST reconstruction using principal component analysis. *Magn Reson Med* 2009;**62**:706–16.